Materials Transactions, Vol. 51, No. 3 (2010) pp. 548 to 552

Nondestructive Observation of Pore Structures of A1050 Porous Aluminum Fabricated by Friction Stir Processing

Yoshihiko Hangai[1], Yuichiro Ozeki[1,*1], Shigehiro Kawano[1,*2], Takao Utsunomiya[2], Osamu Kuwazuru[3], Makoto Hasegawa[4], Shinji Koyama[1] and Nobuhiro Yoshikawa[5]

[1]*Department of Mechanical System Engineering, Graduate School of Engineering, Gunma University, Kiryuu 376-8515, Japan*
[2]*Research Organization for Advanced Engineering, Shibaura Institute of Technology, Saitama 337-8570, Japan*
[3]*Department of Nuclear Power and Energy Safety, Graduate School of Engineering, University of Fukui, Fukui 910-8507, Japan*
[4]*Division of Materials Science and Engineering, Graduate School of Engineering, Yokohama National University, Yokohama 240-8501, Japan*
[5]*Institute of Industrial Science, The University of Tokyo, Tokyo 153-8505, Japan*

In the automotive industry, porous aluminum is expected to be used as a new functional material because of its light weight, high energy absorption and high sound-insulating property. Recently, a new processing route for fabricating the porous aluminum precursor, which utilizes friction stir processing (FSP), has been developed. It is expected that, by applying the FSP route precursor method, the cost-effective fabrication of porous aluminum with high productivity can be realized. In this study, two different types of A1050 porous aluminum were fabricated from two different sizes of precursor by the FSP route precursor method. The two types of porous aluminum fabricated using small and large precursors are hereafter referred to "FSP-S porous aluminum" and "FSP-L porous aluminum", respectively. The pore structures of FSP-S porous aluminum, FSP-L porous aluminum and also commercially available porous aluminum (ALPORAS, fabricated by Shinko Wire Co., Ltd.) were nondestructively observed by X-ray computed tomography (X-ray CT). From the nondestructive observation of pore structures, it was shown that a large number of pores of smaller area and volume were distributed in porous aluminum fabricated by the FSP route precursor method compared with the pores in ALPORAS. However, there was little difference in the circularity of pores between porous aluminum fabricated by the FSP route and ALPORAS, and there was little dependence of the pore structure on the precursor size for porous aluminum fabricated by the FSP route. This result indicates the potential of the FSP route for fabricating larger porous aluminum samples.
[doi:10.2320/matertrans.MBW200921]

(Received October 16, 2009; Accepted January 6, 2010; Published February 17, 2010)

Keywords: *porous metals, friction stir processing, aluminum alloy, pore structure, foam, X-ray computed tomography*

1. Introduction

In the automotive industry, porous aluminum is expected to be used as a new functional material because of its many advantages such as weight reduction enabling low fuel consumption, high crash energy absorption properties for increased safety, and high sound absorption reducing the acoustic emissions from cars and improving their comfort.[1,2)]

Various types of processes have been developed for fabricating porous aluminum including the ALPORAS process,[3)] the Lotus-type process[2)] and the precursor method.[4–11)] A precursor method has high potential for obtaining high-porosity and high-quality (i.e., a uniform pore size distribution with highly spherical pores) closed-cell porous aluminum. In the precursor method, aluminum alloy (as a starting material) and a blowing agent powder are first mixed. This foamable mixture is called the "precursor". Next, the precursor is heat-treated to decompose the blowing agent powder and to release gases. Finally, these gases expand the softened aluminum alloy to form porous aluminum. There are several routes for fabricating the precursor, such as the powder metallurgical route,[4,5)] the ARB process route[6,7)] and the compressive torsion processing route.[8,9)] However, various factors prevent their practical application,[1)] such as the use of expensive aluminum alloy powder for the starting material and the need for many time-consuming and complicated fabrication processes.

Recently, a new processing route for fabricating the precursor, which utilizes friction stir processing (FSP), has been developed.[10,11)] It is expected that, by applying the FSP route precursor method, the cost-effective fabrication of porous aluminum with high productivity can be realized.[10)] However, a quantitative evaluation of the pore structure of porous aluminum fabricated by the FSP route, which affects the properties of porous aluminum, has not been carried out in previous studies.[12,13)] Also, only porous aluminum samples that were too small to be subjected to compression tests[14)] were fabricated in the previous studies.[12,13)]

In this study, two different sizes of A1050 porous aluminum were fabricated from two different sizes (small and large) of precursor by the FSP route precursor method, which we hereafter refer to as "FSP-S porous aluminum" and "FSP-L porous aluminum", respectively. The pore structures of FSP-S porous aluminum, FSP-L porous aluminum and also commercially available porous aluminum (ALPORAS, fabricated by Shinko Wire Co., Ltd., by direct foaming of melts with blowing agents[3)]) were nondestructively observed by X-ray computed tomography (X-ray CT). The following three issues were investigated. First, the pore structures (area and circularity of pores) were investigated by the analysis of two-dimensional cross-sectional X-ray CT images. Next, the volumes of pores were investigated three-dimensionally by stacking two-dimensional cross-sectional X-ray CT images using image-processing software. Finally, the dependence of the pore structure (area, circularity and volume of pores) of FSP-S porous aluminum and FSP-L porous aluminum on the

*1Graduate Student, Gunma University
*2Undergraduate Student, Gunma University

precursor size was investigated. From these results, the feasibility of fabricating larger porous aluminum samples by the FSP route, on which compression tests can be performed, was also examined.

2. Experimental Procedure

2.1 FSP procedure

Figure 1 shows a schematic illustration of the FSP route used in this study. Commercially available pure aluminum A1050 plates of 3 mm and 3.5 mm in thickness were used for the fabrication of FSP-S porous aluminum and FSP-L porous aluminum, respectively. Two aluminum plates were stacked with the blowing agent powder and stabilization agent powder distributed between them. FSP was carried out using an SHH204-720 FSW machine (Hitachi Setsubi Engineering Co., Ltd.). The FSP tool has a columnar shape with a screw probe. The diameter of the tool shoulder is 17 mm, the diameter of the tool probe is 6 mm and its length is 5 mm. SKH51 high-speed tool steel was used as the tool material. The traversing speed of the tool was 100 mm/min and a tilt angle of 3° was used throughout the experiments.

Titanium(II) hydride (TiH_2, <45 μm) powder and alumina (α-Al_2O_3, ~1 μm) powder were used as the blowing agent and stabilization agent, respectively. The stabilization agent was used to stabilize the pore structure and to prevent the release of gases from porous aluminum by improving its viscosity during the foaming process. The powders were placed along the path of the FSP tool, as shown in Fig. 1(a). The amounts used were 1 mass% TiH_2 and 5 mass% Al_2O_3, relative to the mass of aluminum with the dimensions of the area over which TiH_2 and Al_2O_3 were distributed and the length of the tool probe. Multipass FSP[15,16] was applied to thoroughly mix TiH_2 and Al_2O_3 by traversing the same FSP region more than once and to obtain a larger area of precursor by traversing different regions.

2.1.1 FSP procedure of FSP-S porous aluminum

The procedure of multipass FSP applied to fabricate FSP-S porous aluminum was as follows. First, as shown in Figs. 1(c) and (d), FSP was carried out twice in the region where TiH_2 and Al_2O_3 were placed by shifting the FSP tool by approximately the diameter of the tool probe in the direction perpendicular to the FSP direction. Next, as shown in Fig. 1(e), the traversing direction was reversed and the next FSP was carried out twice in exactly the same region as before. Finally, as shown in Figs. 1(f) and (g), the four above-mentioned FSPs (as shown in Figs. 1(c)–(e)) were carried out once again. The tool rotating rate during the traversing of the tool was 1000 rpm throughout the fabrication of each precursor of FSP-S porous aluminum. Precursors of 6 mm thickness, 15 mm width and 15 mm length were machined from the region stirred by FSP.

2.1.2 FSP procedure of FSP-L porous aluminum

The procedure of multipass FSP applied to fabricate FSP-L porous aluminum was as follows. First, as shown in Fig. 1(c′), FSP was carried out four times in the region where TiH_2 and Al_2O_3 were placed by shifting the FSP tool by approximately the diameter of the tool probe in the direction perpendicular to the FSP direction for each FSP. Second, as shown in Fig. 1(d′), the traversing direction was reversed and FSP was carried out four times in exactly the same region as before. Third, as shown in Fig. 1(e′), the plate was turned over, and TiH_2 and Al_2O_3 powders were placed on the reverse side of the FSP surface along the path of the FSP tool. Finally, as shown in Figs. 1(f′) and (g′), the same FSP procedures as those shown in Figs. 1(c′) and (d′) were carried out once again to obtain a thicker precursor. The tool rotating rate during the traversing of the tool was 2200 rpm throughout the fabrication of each precursor of FSP-L porous aluminum. In a previous study, we confirmed that there was

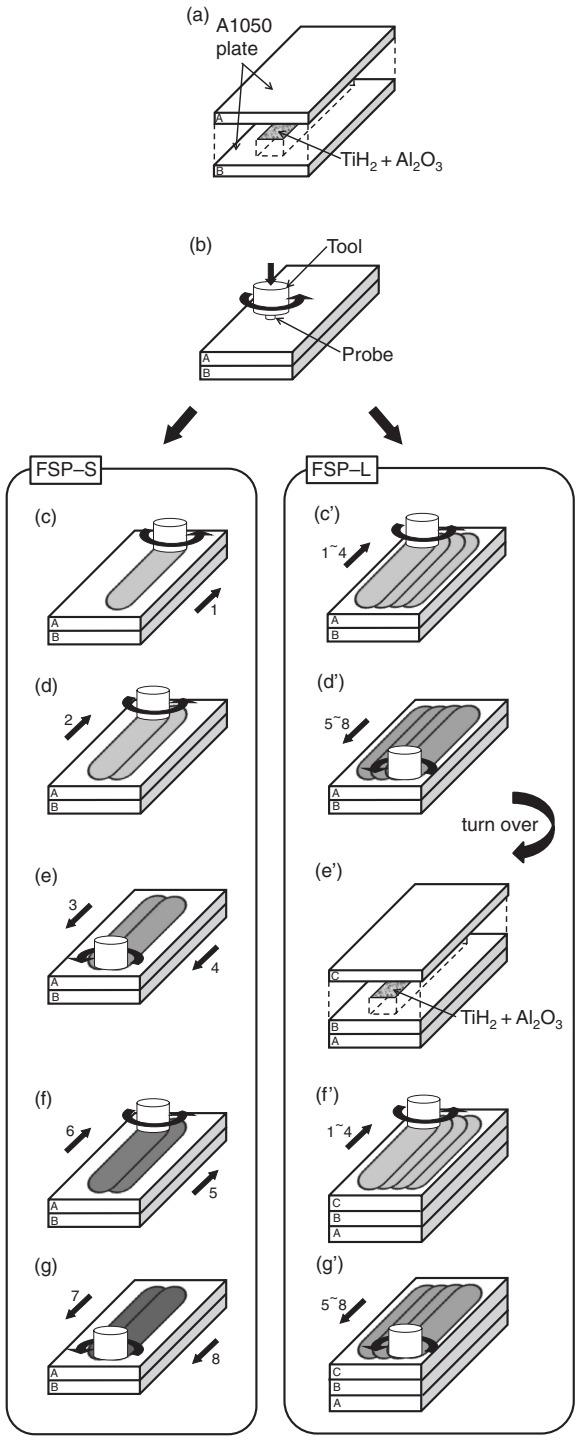

Fig. 1 Schematic illustration of the manufacturing process of precursors of FSP-S porous aluminum and FSP-L porous aluminum by FSP.

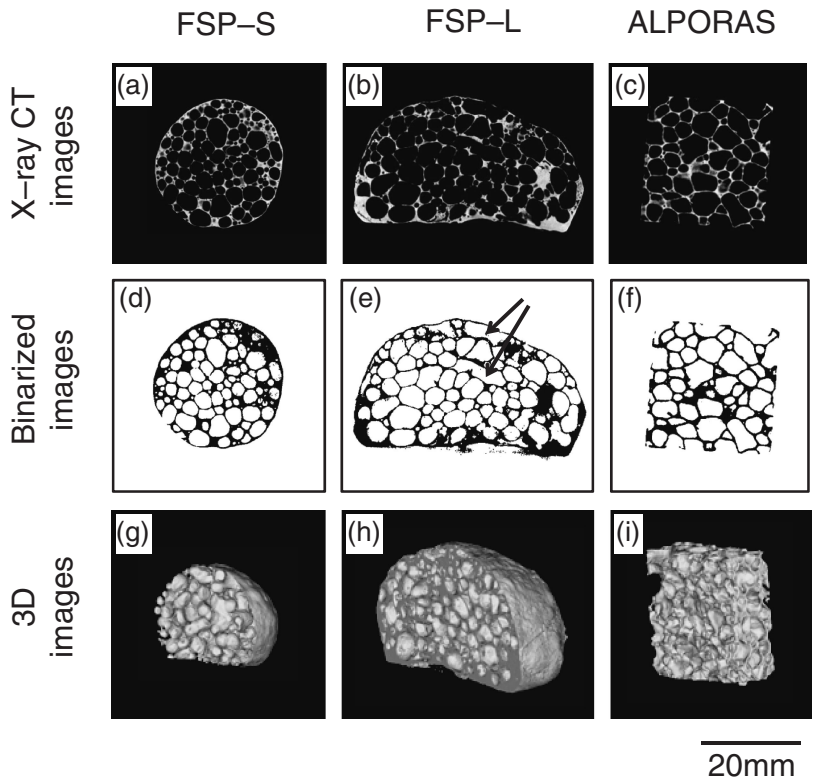

Fig. 2 Two-dimensional cross-sectional X-ray CT images of (a) FSP-L porous aluminum, (b) FSP-S porous aluminum and (c) ALPORAS samples. (d)–(f) Two-dimensional binarized cross-sectional X-ray CT images of the samples in (a)–(c), respectively. (g)–(i) Three-dimensional volume images corresponding to the samples in (a)–(c), respectively.

little difference in the porosity and pore structure obtained at a tool rotating rate of 1000 rpm by traversing the tool four times, as shown in Figs. 1(c)–(g), and those obtained at a tool rotating rate of 2200 rpm by traversing the tool twice, as shown in Figs. 1(c′)–(d′), in the case of A1050 porous aluminum.[13] According to this result, a larger precursor can be made with a similar FSP time to that required for a smaller precursor by increasing the tool rotating rate. Precursors of FSP-L porous aluminum of 10.5 mm thickness, 25 mm width and 25 mm length were machined from the region stirred by FSP.

2.2 Foaming procedure

The precursors were heat-treated in a preheated electric furnace to induce foaming. The holding temperature (equal to the preheated temperature) was determined by reference to our previous study[13] and was fixed at 1003 K during the heating process. The holding time for FSP-S porous aluminum was fixed at 10 min, also in accordance with our previous study,[13] whereas that for FSP-L porous aluminum was varied from 14 to 15 min. The sample was then cooled to room temperature under ambient conditions. Six precursor samples of FSP-S porous aluminum and two precursor samples of FSP-L porous aluminum were foamed.

2.3 Evaluation of pore structures

The porosity p (%) of FSP-S porous aluminum and FSP-L porous aluminum, including the skin, was calculated as

$$p = (\rho_i - \rho_f)/\rho_i \times 100, \quad (1)$$

where ρ_i is the density of the precursor before heating and ρ_f is the density of the foamed aluminum. The densities were evaluated by Archimedes' principle.

The circularity e of the pores was calculated as

$$e = 4\pi A/L^2, \quad (2)$$

where A is the pore area and L is the pore perimeter. A value of circularity closer to 1 indicates a more circular pore.

2.4 X-ray CT inspection

The pores in the foamed aluminum were observed non-destructively by X-ray CT using an SMX-225CT microfocus X-ray CT system (SHIMADZU Corporation) at room temperature. The X-ray source was tungsten. A cone-type CT, which has a three-dimensional image construction system, was employed. In this system, a single rotation of the specimen was sufficient to obtain a three-dimensional volume image, which consists of a set of X-ray CT images with a slice pitch equal to the length of one pixel in the X-ray CT image. The resolution of the X-ray CT image was 512×512, and the length of one pixel was 71.4 μm, 100.0 μm and 78.4 μm for FSP-S porous aluminum, FSP-L porous aluminum and ALPORAS, respectively. The height resolution in each case was about 450. The X-ray CT images displayed 16-bit gray-scale data. The X-ray tube voltage and current were 80 kV and 30 μA, respectively. FSP-S porous aluminum and FSP-L porous aluminum, including their skin, were observed as they foamed. ALPORAS samples were machined to dimensions of 25 mm × 25 mm × 10 mm before observation. To obtain the pore structures, an appropriate

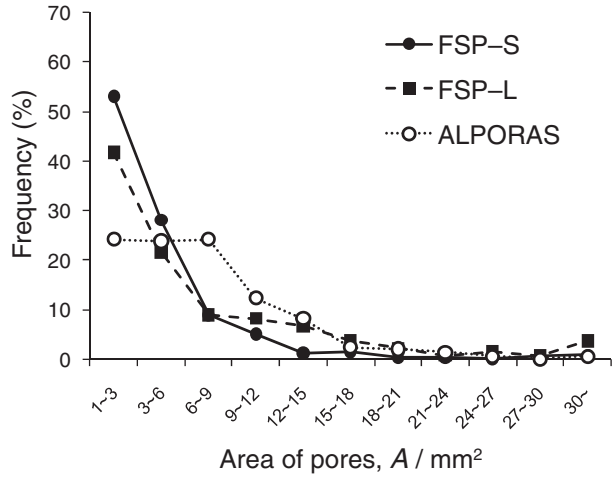

Fig. 3 Relationship between area of pores A and frequency of observation in two-dimensional binarized cross-sectional X-ray CT images.

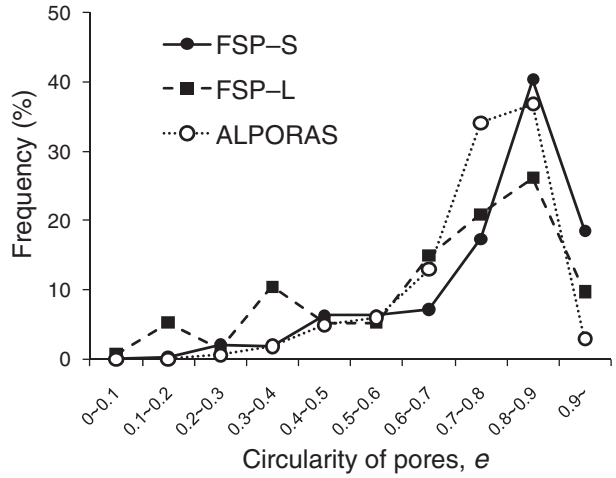

Fig. 4 Relationship between circularity of pores and frequency of observation in two-dimensional binarized cross-sectional X-ray CT images.

threshold was set to distinguish the aluminum and the pores, and binarized X-ray CT images were established. Pores with areas of less than 1 mm^2 were excluded because the resolution of the X-ray CT images did not allow their accurate evaluation.

By stacking the cross-sectional X-ray CT images, three-dimensional volume images were obtained using VOXELCON 2008 image-processing software (Quint Corporation). To obtain the volumes of pores in the three-dimensional images, an appropriate threshold was set to distinguish the aluminum and the pores, and an isosurface was established. Pores with volumes of less than 1 mm^3 were excluded owing to the resolution of the X-ray CT images.

3. Results and Discussion

The mean porosities of FSP-S porous aluminum and FSP-L porous aluminum were 78.4% and 78.7%, respectively. The porosity of ALPORAS was approximately 90%.[3] The difference between these values was due to the existence or nonexistence of a skin.

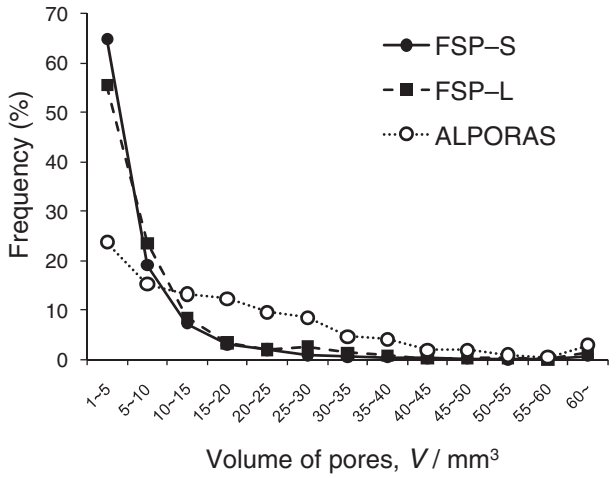

Fig. 5 Relationship between volume of pores V and frequency of observation in three-dimensional X-ray CT volume images.

Figures 2(a)–(c) show cross-sectional X-ray CT images of samples of FSP-S porous aluminum (Fig. 2(a)), FSP-L porous aluminum (Fig. 2(b)) and ALPORAS (Fig. 2(c)). Gray regions indicate the aluminum alloy and black regions indicate pores. Figures 2(d)–(f) show binarized and reversed black and white cross-sectional X-ray CT images of the samples shown in Figs. 2(a)–(c), respectively. Black regions indicate the aluminum alloy and white regions indicate pores. Figures 2(g)–(i) show the three-dimensional volume images corresponding to the samples in Figs. 2(a)–(c), respectively.

Figure 3 shows the relationship between the area of pores A and the frequency of observation in two-dimensional binarized cross-sectional X-ray CT images such as those shown in Figs. 2(d)–(f). The total number of pores evaluated was 335 from six samples of FSP-S porous aluminum, 134 from two samples of FSP-L porous aluminum and 487 from eleven samples of ALPORAS. For FSP-S porous aluminum, the frequency of pores with area less than 3 mm^2 was more than 50%, and the frequency rapidly decreased with increasing pore area. This tendency was also observed for FSP-L porous aluminum. In contrast, for ALPORAS the frequency of pores was approximately 25% for areas of 1–3 mm^2, 3–6 mm^2 and 6–9 mm^2, then gradually decreased with increasing pore area.

Figure 4 shows the relationship between the circularity of pores and the frequency of observation in the two-dimensional binarized cross-sectional X-ray CT images. The numbers of pores evaluated were the same as those for Fig. 3. The frequency was maximum at a circularity of 0.8–0.9 and a similar frequency distribution was obtained for all three types of porous aluminum. However, for FSP-L porous aluminum, the frequencies of low values of circularity such as 0.1–0.2 and 0.3–0.4 were slightly higher. Examples of such pores are indicated by black arrows in Fig. 2(e), and they were generated because of the excessive heating time, which induced the movement and coalescence of pores, causing the generation of elongated pores. Further studies are clearly necessary to optimize the foaming conditions.

Figure 5 shows the relationship between the volume of pores V and the frequency of observation in three-dimen-

sional volume images such as those shown in Figs. 2(g)–(i). The numbers of pores evaluated were 1599 from six samples of FSP-S porous aluminum, 586 from two samples of FSP-L porous aluminum and 820 from eleven samples of ALPORAS. For FSP-S porous aluminum and FSP-L porous aluminum, approximately 60% of pores had a volume of less than 5 mm^3, the frequency decreased with increasing volume, and hardly any pores had a volume exceeding 30 mm^3. In contrast, for ALPORAS, approximately 25% of pores had a volume of less than 5 mm^3, and the frequency gradually decreased with increasing pore volume. The mean pore volumes were 6.56 mm^3, 8.38 mm^3 and 17.87 mm^3 for FSP-S porous aluminum, FSP-L porous aluminum and ALPORAS, respectively. Thus, it was shown that the pores in porous aluminum obtained by the FSP route had a smaller volume with a narrower distribution than those in ALPORAS. This tendency was also observed for pore area in the two-dimensional cross-sectional X-ray CT images, and has also been reported in the literature.[17] Although more pores can be evaluated from each porous aluminum sample using the three-dimensional volume images compared with the two-dimensional cross-sectional images, the above result indicates that two-dimensional cross-sectional observation was satisfactory for comparing the pore structures in porous aluminum obtained by the FSP route and those in ALPORAS in this study.

From these results, it was considered that there was limited dependence of the pore structures in porous aluminum fabricated by the FSP route on the precursor size. Thus, the fabrication of larger samples of porous aluminum with a small pore volume distributed within a narrow range and at least 10 pores for each side,[14] which can be subjected to compression tests, is expected to be possible by the FSP route.

4. Conclusions

Closed-cell A1050 porous aluminum was fabricated by the FSP route precursor method. In this study, the pore structures of fabricated porous aluminum (FSP-S porous aluminum and FSP-L porous aluminum) and commercially available porous aluminum (ALPORAS) were nondestructively observed by X-ray CT inspections, and the area, circularity and volume of pores were compared. The experimental results led to the following conclusions.

(1) A large number of pores of smaller area and volume were distributed in porous aluminum fabricated by the FSP route compared with those in ALPORAS.

(2) There was little difference in the circularity of pores between porous aluminum fabricated by the FSP route and those in ALPORAS.

(3) There was little size dependence of the pore structure of porous aluminum fabricated by the FSP route on the precursor size. This result indicates the possibility of fabricating larger porous aluminum samples by the FSP route.

(4) There was little difference between the trends observed for pore structures using two-dimensional cross-sectional X-ray CT images and those obtained from three-dimensional X-ray CT volume images. This result indicates that two-dimensional cross-sectional observation is satisfactory for evaluating the pore structures in porous aluminum.

Acknowledgments

The authors thank former Assistant Professor T. Yokota, Shibaura Institute of Technology, and Professor K. Saito, Gunma University, for their helpful advice on conducting the experiments, and Professor H. Kumehara, Gunma University, for fruitful discussions throughout this study. This work was financially supported by the Industrial Technology Research Grant Program in 2009 from the New Energy and Industrial Technology Development Organization (NEDO) of Japan.

REFERENCES

1) J. Banhart: Prog. Mater. Sci. **46** (2001) 559–632.
2) H. Nakajima: Prog. Mater. Sci. **52** (2007) 1091–1173.
3) T. Miyoshi, M. Itoh, S. Akiyama and A. Kitahara: Adv. Eng. Mater. **2** (2000) 179–183.
4) H. D. Kunze, J. Baumeister, J. Banhart and M. Weber: Powder Metall. Int. **25** (1993) 182–185.
5) F. Baumgartner, I. Duarte and J. Banhart: Adv. Eng. Mater. **2** (2000) 168–174.
6) K. Kitazono, E. Sato and K. Kuribayashi: Scr. Mater. **50** (2004) 495–498.
7) K. Kitazono, S. Nishizawa, E. Sato and T. Motegi: Mater. Trans. **45** (2004) 2389–2394.
8) S. Tsuda, M. Kobashi and N. Kanetake: Mater. Trans. **47** (2006) 2125–2130.
9) N. Kanetake, M. Kobashi and S. Tsuda: Adv. Eng. Mater. **10** (2008) 840–844.
10) Y. Hangai and T. Utsunomiya: Metall. Mater. Trans. A **40** (2009) 275–277.
11) Y. Hangai and T. Utsunomiya: Metall. Mater. Trans. A **40** (2009) 1284–1287.
12) Y. Hangai, Y. Ozeki and T. Utsunomiya: Mater. Trans. **50** (2009) 2154–2159.
13) Y. Hangai, T. Utsunomiya and M. Hasegawa: Journal of Materials Process. Tech. **210** (2010) 288–292.
14) JIS-H-7902: *Method for compressive test of porous metals*, (Japanese Standards Association, 2008).
15) Y. S. Sato, S. H. C. Park, A. Matsunaga, A. Honda and H. Kokawa: J. Mater. Sci. **40** (2005) 637–642.
16) J. Q. Su, T. W. Nelson and C. J. Sterling: Scr. Mater. **52** (2005) 135–140.
17) K. Kitazono and E. Sato: Materia Japan **45** (2006) 653–656.